Longitudinal, transverse, and perpendicular magnetoimpedance in nearly zero magnetostrictive amorphous alloys

R. L. Sommer* and C. L. Chien
Department of Physics and Astronomy, The Johns Hopkins University, Baltimore, Maryland 21218
(Received 15 November 1995)

Giant magnetoimpedance effects at 100 kHz in three measuring geometries (longitudinal, transverse, and perpendicular) on amorphous $Co_{70.4}Fe_{4.6}Si_{15}B_{10}$, subjected to different field annealings are described. For suitably annealed samples, rich peak features have been observed in longitudinal and perpendicular, but not in transverse, measurements. The results can be understood in terms of the effects of the magnetic annealing and measurement geometries on the effective differential susceptibility of the material.

INTRODUCTION

In the last few years, frequency- and field-dependent impedance has been observed in amorphous materials with nearly zero magnetostriction in ribbons,[1–4] and more recently in highly magnetostrictive wires,[5] and thin films.[6] The origin of the pronounced magnetoimpedance (MI) effects appears to be the field dependence of the effective transverse permeability, which is better understood in the case of amorphous wires.[2] Very recently,[4] we reported the effects of field-annealing geometry, highlighting the role of transverse anisotropy on the longitudinal MI (LMI) of the near-zero magnetostriction amorphous $Co_{70.4}Fe_{4.6}Si_{15}B_{10}$ ribbons. However, many questions concerning the nature of the effect and the rich spectra of the MI effects remain to be addressed.

A key question is the effect of the measurement geometry on the MI. Early reports for transverse MI (TMI) describe a very insignificant effect.[1,3] We show in this work that the TMI effects not only exist, they have the same order of magnitude as that of the LMI. Furthermore, we have also observed perpendicular magnetoimpedance (PMI), which exhibits the same features as the LMI. The effects of the field annealing in all three measurement geometries have been studied. Equally significant, we show that LMI, TMI, and PMI effects occur in very different field ranges due to the role of the demagnetization factors on the specific components of the differential permeability of the material. The mechanisms that contribute to the rich peak structure of the LMI and PMI have also been indicated.

EXPERIMENT

We have used amorphous $Co_{70.4}Fe_{4.6}Si_{15}B_{10}$ ribbon samples, a well-known amorphous alloy with nearly zero magnetostriction. The ribbon, made by standard melt-spinning method, has a reasonably uniform thickness (18 ± 1 μm) and a resistivity of about 122 $\mu\Omega$ cm. Ribbons with a large variation of thickness may compromise reliable measurements and complicate interpretations. Samples from adjacent regions of the same 12.5 mm wide ribbon were cut into sections of about 10×1 mm^2. Four-terminal MI measurements with In metal contacts were used. Current (at the frequency of 100 kHz, 20 mA peak) was provided by a low noise current source, and the signal detected by an SR830 dual-phase lock-in amplifier. The MI results are expressed in terms of the impedance $Z(H)=R(H)+jX(H)$.

The probe current was applied along the long direction of the sample. In the LMI and TMI measurements, the dc magnetic field is applied in the ribbon plane, parallel and perpendicular, respectively, to the probe current. In the PMI geometry, the dc field is perpendicular to the sample plane and the probe current. The dc magnetic field was provided by a long solenoid for the LMI and TMI measurements with a maximum field of 150 Oe and a field uniformity better than 2% over the sample's length. For the PMI measurements, the field was provided by an electromagnet with fields up to 5 kOe. Magnetic annealing at $T_A=300$ °C was performed in flowing Ar gas with either 0 or 2 kOe field applied in the sample plane, oriented either parallel to the long direction [longitudinal annealing (LA)] or along the short direction [transverse annealing (TA)] of the samples. One sample was kept as cast (AC) without annealing and another was annealed in zero field (ZFA). In what follows, the MI effect will be expressed as $\Delta R/R(H_{\max})$ and $\Delta X/R(H_{\max})$, where $H_{\max}=2$ kOe for PMI and $H_{\max}=150$ Oe for LMI and TMI.

RESULTS AND DISCUSSIONS

In Fig. 1 the longitudinal magnetoimpedance (LMI) results for the samples subjected to different annealing geometries (AC, ZFA, LA, and TA mentioned above) are shown. There is a large LMI effect in the AC sample [Fig. 1(a)], showing roughly two round peaks. Upon annealing at zero field, the magnitude of the effect decreases significantly [Fig. 1(b)]. Longitudinal annealing produces a small effect [see Fig. 1(c)] and the overall shape is a wide plateau with no resolvable peak. Transverse annealing recovers the large MI effect [Fig. 1(d)] with very well-defined peak structure. It may be noted that most of the LMI occurs in very low fields, in the range of only ±10 Oe. As shown in Fig. 1, regardless of the annealing conditions, the MI effect for the reactance part $(\Delta X/R)$ is larger than that of the resistance part $(\Delta R/R)$. The TA sample is the only exception.

It should be mentioned that in Figs. 1(a)–1(c), the decreasing-field curves (not shown) and the increasing-field curves (shown) are essentially the same. In Fig. 1(d), however, while the two shoulder peaks at ±6 Oe are reversible, the central peal is hysteretic; the central peak at 2 Oe in Fig.

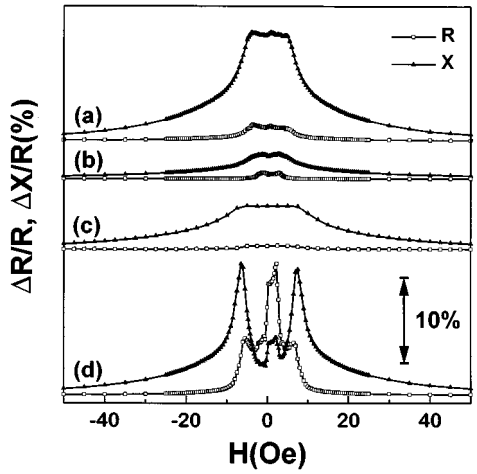

FIG. 1. Longitudinal magnetoimpedance (LMI) results at $f=100$ kHz and 20 mA peak probe current of (a) as-cast sample and samples subjected to different annealing conditions at $T_A=300$ °C: (b) at $H_A=0$, (c) longitudinally annealed at $H_A=2$ kOe, and (d) transversely annealed at $H_A=2$ kOe. The results are expressed as $\Delta R/R(H_{\max})$ and $\Delta X/R(H_{\max})$. All graphs share the same vertical scale indicated by the 10% mark.

1(d) appears at -2 Oe in the decreasing-field curve.

In Fig. 2, the results of the transverse magnetoimpedance (TMI) for the same samples of Fig. 1 are shown. A large effect is again observed in the AC sample [Fig. 2(a)], which shows a bell-shaped curve without many of the details present in the LMI. For the ZFA sample [Fig. 2(b)], the magnitude of the effect is much smaller than the AC case, in a way consistent with the LMI. For the LA sample [Fig. 2(c)], the TMI shows broad peaks in the resistance and reactance curves. For the TA sample [Fig. 2(d)], the large effect in TMI is again retrieved, in a manner similar to that of the LMI. The reactive part (X) was again found to be larger than the resistance (R), except in the case of the TA sample. In all cases, TMI spectra are very broad with essentially no resolved features.

Figure 3 shows the results for the perpendicular magnetoimpedance (PMI). All the features observed for the LMI are also present in the PMI. The PMI shown in Figs. 3(a)–

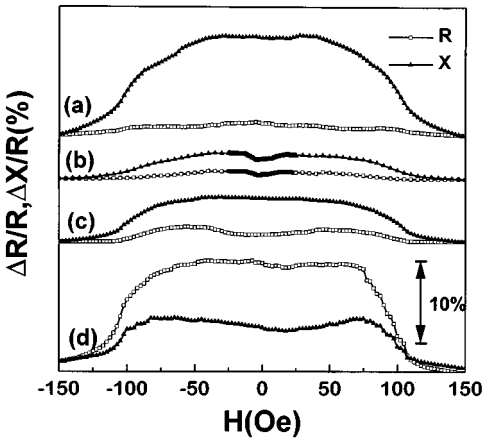

FIG. 2. Transverse magnetoimpedance (TMI) for the same samples shown in Fig. 1.

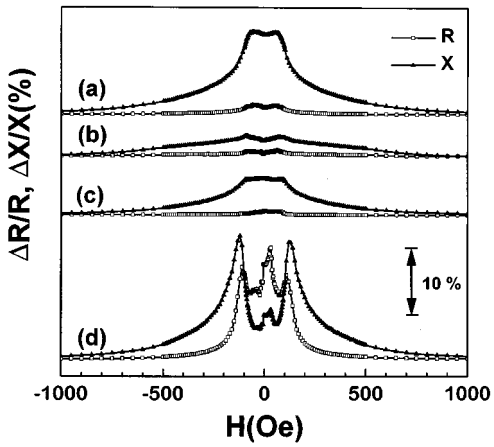

FIG. 3. Perpendicular magnetoimpedance (PMI) for the same samples shown in Fig. 1.

3(c) are nonhysteretic, whereas the result for the TA sample [Fig. 3(d)] is hysteretic, where the central peak exhibits the same hysteresis as observed for the LMI [Fig. 1(d)].

It is important to note the differences among LMI, TMI, and PMI shown, respectively, in Fig. 1, Fig. 2, and Fig. 3. First of all, the field ranges in which substantial MI effects exist are very different in the three cases. The field range in TMI (about 2 ± 100 Oe) is about one order of magnitude larger than that of LMI (about ±10 Oe). The field range in PMI is large still at about ±400 Oe. If one were guided by the LMI results shown in Fig. 1 and attempted to measure TMI using only small external fields, one would not have observed a large TMI effect. This may explain why TMI, with magnitude similar to that of LMI, was not reported earlier.[1,3] The same situation applies to the case of PMI, which exhibits features similar to the LMI case but occurring in a field range more than one order of magnitude higher. Second, the TMI results exhibit practically no peak structure, whereas LMI and PMI do. Third, of the four annealed and nonannealed samples, only the transverse annealed samples in LMI and PMI [Fig. 1(d) and Fig. 3(d)] reveal the detailed peak structure with which one can elucidate the mechanisms for the MI effects. This comparison demonstrates vividly that the most desirable measurement geometry is LMI and the most useful samples are those subjected to transverse field annealing.

The differences among the LMI, TMI, and PMI measurements can be understood in terms of the effect of the annealing and measurement geometry on the effective differential permeability, which is the underlying quantity responsible for the MI effects. It is well accepted that for the LMI observed in high permeability materials, the relevant parameter is the skin depth length: $\delta_m=c/\sqrt{2\pi\omega\sigma\mu_{\text{eff}}}$, where σ and μ_{eff} are the conductivity and the effective differential permeability of the material, ω the angular frequency, and c is the speed of light.[2] If the ribbon thickness is larger than $\delta_m/2$, the frequency and field dependence of the impedance is $Z\propto\sqrt{f\mu_{\text{eff}}(H,f,I)}$, where f is the frequency, I the probe current, and $\mu_{\text{eff}}(H,f,I)$ is the dependence of μ_{eff} on frequency, field, and current. It can be immediately seen that the field and frequency dependence of the differential permeability $\mu_{\text{eff}}=1+\chi_{\text{eff}}$ play a central role in defining the magnitude of the MI and the peak structure observed.

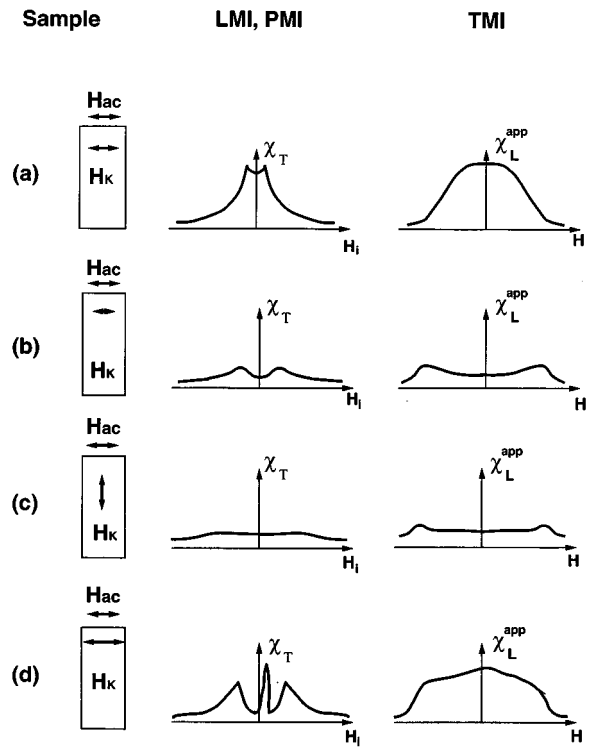

FIG. 4. Schematics showing the effects of annealing, measurement geometries, and induced anisotropies on longitudinal (LMI), transverse (TMI), and perpendicular (PMI) magnetoimpedance for (a) as-cast, (b) annealed at zero field, (c) longitudinally annealed, and (d) transversely annealed samples. The relevant transverse susceptibility (second column) for LMI and PMI and apparent longitudinal susceptibility for TMI (third column) are also shown. The LMI and PMI are very similar if plotted as a function of the respective internal field H_i.

In the following, we provide a coherent description of the MI effects that accounts for all the features of LMI, TMI, and PMI, as well as their dependence on the annealing geometries. We first discuss the annealing geometries. We recall the random nature of the magnetic anisotropy in amorphous systems. It is a well-known fact that the as-cast amorphous samples already have a small amount of anisotropy induced during the fabrication process, with an effective anisotropy field of H_K.[7] The evolution of the effective anisotropy field, as a result of annealing is schematically shown in the left column of Fig. 4. Annealing with or without an external field manipulates the magnitude and direction of the effective field, as schematically shown in Fig. 4. Upon annealing in zero field [Fig. 4(b)], part of this anisotropy is relaxed, but not eliminated. A component of the anisotropy perpendicular to the long direction is still present, as indicated in Fig. 4(b). For the longitudinally annealed sample [Fig. 4(c)], a larger part of the anisotropy is now parallel to the long direction of the sample, whereas in the case of the transverse-annealed sample [Fig. 4(d)], a larger part of the anisotropy is induced perpendicular to the long direction of the sample.

In all MI measurements, the probe current is along the long direction of the sample. The ac field (H_{ac}) produced by the probe current is always transverse to the long direction of the sample as shown in the left column of Fig. 4. The geometry of the MI measurement defines which permeability (or susceptibility) is important for the MI. In all LMI measurements, the field produced by the probe current (H_{ac}) is perpendicular to the applied dc field H. The relevant susceptibility for LMI is the transverse susceptibility (χ_T). On the other hand, in TMI measurements, the field produced by the probe current (H_{ac}) and the applied dc field H are parallel, thus, the longitudinal susceptibility (χ_L) is the relevant one.[8] In other words, the transverse and longitudinal susceptibility are relevant, respectively, to longitudinal and transverse MI. For the PMI, using the same reasoning, the relevant susceptibility is the transverse one, same as that of LMI.

As indicated previously, the MI spectra reflect the field dependence of the relevant permeability (or susceptibility), and hence the peak structures in the MI. They are the results of the relative orientation of the field generated by the probe current (H_{ac}), the anisotropy field (H_K), and the applied dc field (H), the last of which is subject to demagnetization correction. The internal fields for the three measuring geometries are given approximately by $H_i^{\nu}=H-4\pi D_{\nu}M_{\nu}$, where $\nu=L$, T, and $\perp$ correspond to the longitudinal, transverse, and perpendicular directions of the sample. In the second column of Fig. 4, the behavior of χ_T vs H_i curve, relevant to LMI and PMI is shown for each geometry. The demagnetization field in LMI has a negligible contribution to the internal field because D_L is small. In the case of PMI, the demagnetization expands the H scale for the peak features because D_T is large. In both cases, however, the MI magnitudes and features are hardly influenced by the demagnetizing effects because the magnetization processes responsible for the MI are perpendicular to the average dc magnetization. As a consequence, the LMI and PMI provide the actual internal field dependence of χ_T, with which one can unravel the processes that contribute to the peak structure of the LMI and χ_T.

For TMI, the longitudinal susceptibility χ_L is of relevance. In this case, the demagnetization field has a large effect; it not only influences the internal field, but more importantly, it also places a limit for the longitudinal susceptibility χ_L.[9] The apparent susceptibility is given by $\chi_L^{app}=\chi_L/(1+4\pi D_T\chi_L)$, which is χ_L corrected for demagnetizing effects. In the limit that χ_L is large, the apparent susceptibility will be given by $\chi_L^{app}\sim 1/4\pi D_T$, which together with the smaller internal field, produce the bell-shaped curves for the transverse MI measurements over a large range of applied field H as shown in the third column of Fig. 4. The strong demagnetization effects will always be present in the TMI, regardless of the details of the field dependence of the differential susceptibility or the annealing geometry. The field dependence of the intrinsic χ_L is therefore masked.

Having accounted for all the features of LMI, TMI, and PMI in various samples, annealed or otherwise, we now discuss the peak structures, principally the sample after transverse field annealing. As mentioned earlier, the as-cast sample already has anisotropy.[7] It is well known that after transverse annealing, the transverse susceptibility (χ_T) develops a peak at $H=H_K$.[8,10] We therefore identify the shoulder peaks in Fig. 1(d), located at ± 6 Oe, as H_K (in the case of the PMI, the effect of the demagnetizing field has to be included). The central peaks in the transverse-annealed sample can be attributed to a maximum in the permeability associated with the domain wall structure, known to exist in

amorphous samples after transverse annealing.[8,10] This identification is consistent with the fact that the central peaks, located at ± 2 Oe, are hysteretic, as mentioned earlier. The susceptibility can be described as $\chi = \chi_{DW} + \chi_{rot}$, where χ_{DW} is the susceptibility associated with the domain wall motion and χ_{rot} is the susceptibility associated with the magnetization rotation process. This hypothesis can be tested by high-frequency measurements, because these susceptibilities (χ_{DW} and χ_{rot}) have different attenuation constants due to their different nature. In metallic samples, including amorphous materials, DW motion is attenuated at lower frequencies, when compared with the rotation process. These features have indeed been observed as reported elsewhere.[11]

Finally, it may be mentioned that the results and interpretation reported in this work, intended for the $Co_{70.4}Fe_{4.6}Si_{15}B_{10}$ alloy, are rather general and can be used to understand the effect of the geometry of measurement on the MI of any high permeability material with well-defined magnetic anisotropy axis.

In summary, we have observed transverse (TMI) and perpendicular magnetoimpedance (PMI), in addition to longitudinal MI previously observed, in samples subjected to various field annealings. All LMI, TMI, and PMI measurements show similarly large effect sizes, but occurring in different field ranges and with different peak structures. The rich MI spectra can be understood by identifying the relevant susceptibility in each case, the ac field due to the probe current, and the demagnetization effects associated in each case. The TMI has poorer resolution when compared with LMI and PMI. The LMI spectra, hardly influenced by the demagnetization effects, have the highest sensitivity at the lowest fields. The transverse field annealed sample reveals two main mechanisms: magnetization rotation and domain wall motion, for the MI effects.

ACKNOWLEDGMENTS

The support of ONR Grant No. N00014-91-J-1633 and from CNPq of Brazil are greatly appreciated. The authors thank Dr. R. Hasegawa from AlliedSignal Inc. for providing the $Co_{70.4}Fe_{4.6}Si_{15}B_{10}$ ribbons.

*Permanent address: Departamento de Física UFSM, 97119-900 Santa Maria RS, Brazil.

[1] F. L. A. Machado, C. S. Martins, and S. M. Rezende, Phys. Rev. B **51**, 3926 (1995).

[2] L. V. Panina, K. Mohri, T. Uchiyama, and M. Noda, IEEE Trans. Magn. **31**, 1249 (1995).

[3] R. S. Beach and A. E. Berkowitz, J. Appl. Phys. **76**, 6209 (1994).

[4] R. L. Sommer and C. L. Chien, Appl. Phys. Lett. **67**, 857 (1995).

[5] M. Knobel, M. L. Sánchez, C. Gómez-Palo, and A. Hernando, J. Appl. Phys. (to be published).

[6] R. L. Sommer and C. L. Chien, Appl. Phys. Lett. **67**, 3346 (1995).

[7] H. Fujimori, in *Amorphous Metallic Alloys*, edited by F. E. Lubosrky (Butterworths, London, 1983), p. 300.

[8] H. Hoffman, Phys. Status Solidi **33**, 175 (1969).

[9] R. L. Sommer and C. L. Chien, J. Appl. Phys. (to be published).

[10] W. D. Doyle, X. He, and P. Tang, J. Appl. Phys. **73**, 5995 (1993).

[11] R. L. Sommer and C. L. Chien, J. Appl. Phys. (to be published).